Synthesis, Spectral Characterization, and Structural Studies of 2-Aminobenzoate Complexes of Divalent Alkaline Earth Metal Ions: X-ray Crystal Structures of $[Ca(2\text{-aba})_2(OH_2)_3]_\infty$, $[\{Sr(2\text{-aba})_2(OH_2)_2\}\cdot H_2O]_\infty$, and $[Ba(2\text{-aba})_2(OH_2)]_\infty$ (2-abaH = $2\text{-}NH_2C_6H_4COOH$)†

Ramaswamy Murugavel,* Vivek V. Karambelkar, Ganapathi Anantharaman, and Mrinalini G. Walawalkar

Department of Chemistry, Indian Institute of Technology—Bombay, Powai, Mumbai 400 076, India

Received July 27, 1999

Reactions of alkaline earth metal chlorides with 2-aminobenzoic acid (2-abaH) have been investigated. The treatment of $MCl_2\cdot nH_2O$ (M = Mg, Ca, Sr or Ba) with 2-abaH in a 1:2 ratio in a $MeOH/H_2O/NH_3$ mixture leads to the formation of anthranilate complexes $[Mg(2\text{-aba})_2]$ (**1**), $[Ca(2\text{-aba})_2(OH_2)_3]_\infty$ (**2**), $[\{Sr(2\text{-aba})_2(OH_2)_2\}\cdot H_2O)]_\infty$ (**3**), and $[Ba(2\text{-aba})_2(OH_2)]_\infty$ (**4**), respectively. Alternatively, these products can also be obtained starting from the corresponding metal acetates. Anthranilate complexes **1**−**4** have been characterized with the aid of elemental analysis, pH measurements, thermal analysis, and infrared, ultraviolet, and NMR (^1H and ^{13}C) spectroscopic studies. All the products are found to be thermally very stable and do not melt on heating to 250 °C. Thermal studies of complexes **2**−**4**, however, indicate the loss of coordinated and lattice water molecules below 200 °C. In the case of the magnesium complex, the analytical and thermogravimetric studies indicate the absence of any coordinated or uncoordinated water molecules. Further, the solid-state structures of metal anthranilates **2**−**4** have been established by single-crystal X-ray diffraction studies. While the calcium ions in **2** are heptacoordinated, the strontium and barium ions in **3** and **4** reveal a coordination number of 9 apart from an additional weak metal−metal interaction along the polymeric chains. The carboxylate groups show different chelating and bridging modes of coordination behavior in the three complexes. Interestingly, apart from the carboxylate functionality, the amino group also binds to the metal centers in the case of strontium and barium complexes **3** and **4**. However, the coordination sphere of **2** contains only O donors. All three compounds form polymeric networks in the solid state with the aid of different coordinating capabilities of the carboxylate anions and O−H···O and N−H···O hydrogen bonding interactions.

Introduction

The chemistry of the alkaline earth metals has until recently remained a largely underdeveloped area of the periodic table. There have been a few studies in recent years of the coordination chemistry of these metals in both aqueous and nonaqueous media.[1−5] Magnesium and calcium are biologically *essential elements*, and it has been suggested that these elements were in fact involved with some of the earliest forms of life because of their important role in DNA and protein synthesis.[6] They play an essential role in the activation of enzymes, complexation with nucleic acids, nerve impulse transmission, muscle contraction, and the metabolism of carbohydrates.[7−10] While these two metals are the biologically most important alkaline earth metals, barium and strontium metals have been known as antagonists for potassium and calcium, respectively.[11]

Magnesium and calcium play quite different roles in the body, and this may possibly be due to magnesium having a higher charge-to-radius ratio. This results in a stable hydrated $[Mg(H_2O)_6]^{2+}$ octahedral cation existing in a wide range of magnesium complexes. Further, the larger size of Ca^{2+} ion results in a coordination number of greater than 6 in its complexes. In view of their widespread occurrence in the body and in nature (e.g., magnesium in chlorophyll and calcium in hydroxyapatite in bone, thermolysin, or protein kinase C),[12] a range of model complexes containing Mg^{2+} and Ca^{2+} cations have previously been prepared as probes to elucidate the mode of binding of these metals in vivo and in vitro.[13,14] Such studies

† Dedicated to Professor P. Natarajan on the occasion of his 60th birthday.

* To whom correspondence should be addressed. Phone: +(22) 576 7163 or 576 8163. Fax: +(22) 578 3480. E-mail: rmv@chem.iitb.ernet.in.

(1) McCormick, M. J.; Moon, K. B.; Jones, S. R.; Hanusa, T. P. *J. Chem. Soc., Chem. Commun.* **1990**, 778.
(2) Hitchcock, P. B.; Lappert, M. F.; Lawless, G.; Royo, B. *J. Chem. Soc., Chem. Commun.* **1990**, 1141.
(3) Drake, S. R.; Anderson, K. D.; Hursthouse, M. B.; Malik, K. M. A. *Inorg. Chem.* **1993**, *32*, 1041.
(4) Westerhausen, H. *Inorg. Chem.* **1991**, *30*, 90.
(5) Wojtczak, W. A.; Fleig, P. F.; Hampden-Smith, M. J. *Adv. Organomet. Chem.* **1996**, *40*, 215.
(6) Abdulla, M.; Behbehani, A.; Dashli H. *Magnesium Health Disease* **1989**, 111.
(7) Classen, H. G.; Nowitski, S.; Schimatschek, H. F. *Magnesium Bull.* **1991**, *132*, 39.
(8) Evans, C. A.; Guerremont, R.; Rabenstein, D. L. *Metal Ions In Biological Systems*; Sigel, H., Ed.; Marcel Dekker: New York, NY, 1979; Vol. 9, p 41.
(9) Doyne, T. *Adv. Protein Chem.* **1966**, *22*, 600.
(10) Freeman, H. C. *Inorganic Biochemistry*; Eichhorn, J., Ed.; Marcel Dekker: New York, NY, 1979; Vol. 1, p 129.
(11) (a) Schmidbaur, H.; Mikulick, P.; Müller, G. *Chem. Ber.* **1990**, *123*, 1599. (b) Jenden, D. J.; Reger, J. F. *J. Physiol. (London)* **1963**, *169*, 889. (c) Martin, R. B. In *Metal Ions in Biological Systems*; Siegel, H., Ed.; Marcel Dekker: New York, NY, 1986; Vol. 20, p 43.
(12) Timkovich, R.; Tulinsky, A. *J. Am. Chem. Soc.* **1969**, *91*, 4430.
(13) Schmidbaur, H.; Classen, H. G.; Helbig, J. *Angew. Chem.* **1990**, *102*, 1122. Schmidbaur, H.; Classen, H. G.; Helbig, J. *Angew. Chem., Int. Ed. Engl.* **1990**, *29*, 1090 and references therein.
(14) Schmidbaur, H.; Bach, I.; Wilkinson, D. L.; Müller, G. *Chem. Ber.* **1989**, *122*, 1433.

10.1021/ic990895k CCC: $19.00
Published on Web 03/04/2000

are of fundamental importance in aiding our understanding of the problems of magnesium and calcium deficiency in the human body arising from controlled diet and modern food habits.[13,15] These studies have focused in particular on the use of aspartate, glutamate, orontate, or pyroglutamate ligands.[13]

Schmidbaur,[16] Drake,[3] and others[17,18] have recently unraveled the coordination behavior of salicylic acid toward the group 2 metal cations in the solid state. Salicylates have found widespread application both as antiseptics and as medicinal agents, and studies of hydrated salicylates been primarily initiated to improve our understanding of the modes of coordination of this ligand to a wide range of metal ions. Salicylic acid (salH) has been noted to be one of the simplest models for humic substances in natural waters.[19] Structural studies have revealed that beryllium forms a monomeric four-coordinate salicylate complex, $[Be(Sal)(H_2O)_2]$,[16] whereas magnesium quite predictably forms a regular octahedral complex.[3,17] The heavier metals calcium and strontium form isostructural oligomeric hydrogen-bonded networks of $[M(Sal)_2(H_2O)_2]$.[18]

While structural information is now available for all group 2 metal salicylates except barium, surprisingly no serious efforts have been made thus far to isolate the corresponding anthranilate complexes of these metal ions and structurally characterize them in the solid state.[20] Studies of anthranilic acid complexes also assume importance because it is an important precursor to tryptophan, which is one of the 20 biologically important α-amino acids. Because of this reason, anthranilate complexes of different transition metal ions have been somewhat but inconclusively probed by spectroscopic studies,[21−24] and only recently, the X-ray crystal structures of the Cu^{2+},[25] Zn^{2+},[26] Y^{2+},[27] and Sn^{4+},[28,29] complexes have been determined. The first report on the group 2 metal anthranilates appeared in 1960,[21] which concerns the synthesis and the ultraviolet and infrared spectral studies of Mg, Ca, Sr, and Ba complexes. On the basis of the spectral studies, the authors have interpreted the structures of the group 2 metal anthranilate complexes to be trans square-planar chelate complexes, although the larger group 2 metal ions normally extend their coordination sphere to as many as 10 ligands. The authors have, in particular, not taken into consideration the possibility of coordination of solvent water molecules to the larger group 2 metal dications. Later, D'Avignon and Brown reported on the NQR spectra of these complexes assuming a trans square-planar geometry for these complexes.[22]

Scheme 1

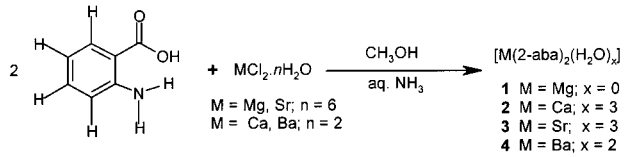

With the aim to further probe the *actual* structures and the spectroscopic properties of these complexes, we have now undertaken a complete study of the synthesis and isolation of the group 2 metal complexes in the solid state, spectroscopic characterization, thermal behavior, and as well as single-crystal X-ray molecular structure determinations of the calcium, strontium, and barium complexes. The results obtained in this study are reported in this paper.

Results and Discussion

Synthesis. The syntheses of title compounds **1**−**4** were accomplished by the reaction of $MCl_2 \cdot nH_2O$ (M = Mg, Ca, Sr, or Ba) with 2-abaH under basic conditions (pH ≈ 10) from an aqueous solution (Scheme 1). Addition of aqueous NH_3 was necessary for the completion of the neutralization of the amino acid, as has been found in the case of salicylate complexes of alkaline earth metal ions.[3] In a general procedure, to a stirred H_2O/methanol solution of the metal halide and the anthranilic acid, an excess of aqueous ammonia solution was added slowly and the volume of the reaction mixture was reduced to half its original volume in a water-bath and filtered. Leaving the resultant clear solution for several days results in the precipitation of large crystals of compounds **2**−**4**. However, addition of ammonia to a mixture of $MgCl_2 \cdot 6H_2O$ and anthranilic acid results in the precipitation of copious amounts of **1** instantaneously. Compound **1** is insoluble in almost all common solvents, and hence, it has not been possible to crystallize this compound. In contrast, compounds **2**−**4** are highly soluble in water and are sparingly (to moderately) soluble in other solvents such as methanol, ethanol, and dimethyl sulfoxide.

Although Hill and Curran employed a similar synthetic route (sodium anthranilate + metal chloride), the isolated products were analyzed to be $[M(2\text{-aba})_2]$ (M = Ca, Sr, or Ba) with no coordinated water molecules.[21] Further, these authors report that the Mg complex is freely soluble in ethanol, whereas the product obtained by the same procedure by us is practically insoluble in most solvents, although our product was also analyzed to have the same $[Mg(2\text{-aba})_2]$ formula.

Analytical Data. The anthranilate complexes **1**−**4** have been obtained in good yield (65−85%) in analytically pure form. The compounds do not melt or decompose below 250 °C. In all cases, the empirical formula and composition of the products could easily be established from the analytical data listed in Table 1. Except in the case of **1**, the data account for the presence of additional coordinated or uncoordinated water molecules. For example, while the observed values for **2**, **3**, and **4** fit very well for a 1:2 complex with three, three, and one water molecule, respectively, the analytical data obtained for **1** indicate a 1:2 complex without any coordinated water molecules, as reported by Hill and Curran.[21] To further verify a simple 1:2 M/L formulation for **1**, apart from repeatedly determining the analytical data, the synthesis of the compound was carried out using other bases such as NaOH or KOH in place of aqueous ammonia. However, in all cases, the resultant product yielded the same analytical data. However, this observation is contrary

(15) Classen, J.; Achilles, W.; Bachem, G. M.; Conradt, A.; Fehlinger, R.; Gossmann, H. H.; Günther, T.; Münzenberg, K. J.; Paschen, K.; Schreiber, G.; Schroll, A.; Spälting, L.; Wischnik, A.; Zumkley, H. *Magnesium Bull.* **1986**, *8*, 117.
(16) Schmidbaur, H.; Kumberger, O.; Riede, J. *Inorg. Chem.* **1991**, *30*, 3101.
(17) Cole, L. B.; Holt, E. M. *Inorg. Chim. Acta* **1989**, *160*, 195.
(18) Debuyst, P. R.; Dejehet, F.; Dekandelaer, M.-C.; Declercq, J.-P.; Germain, G.; Meerssche, M. V. *J. Chim. Phys.* **1979**, *76*, 1117.
(19) Maeda, M.; Murata, Y.; Ito, K. *J. Chem. Soc., Dalton Trans.* **1987**, 1853.
(20) A dinuclear calcium dicarboxylate complex has been recently reported. The dicarboxylic acid used in this study is derived from the condensation of anthranilic acid with dimethylmalonyl chloride. Ueyama, Y.; Takeda, J.; Yamada, Y.; Onoda, A.; Okamura, T.; Nakamura, A. *Inorg. Chem.* **1999**, *38*, 475.
(21) Hill, A. G.; Curran, C. *J. Phys. Chem.* **1960**, *64*, 1519.
(22) D'Avignon, D. A.; Brown, T. L. *Inorg. Chem.* **1982**, *21*, 304.
(23) Rao, T. V. R. K.; Yadav, R. P. *J. Ind. Chem. Soc.* **1992**, *69*, 852.
(24) Prasad, S.; Srivastava, K. P. *J. Ind. Chem. Soc.* **1958**, *35*, 653.
(25) Lange, B. A.; Haendler, R. A.; Haendler, H. M. *J. Solid State Chem.* **1975**, *15*, 325.
(26) Boudreau, S. M.; Boudreau, R. A.; Haendler, H. M. *J. Solid State Chem.* **1983**, *49*, 379.
(27) Boudreau, S. M.; Haendler, H. M. *J. Solid State Chem.* **1981**, *36*, 190.
(28) Narula, S. P.; Bhardwaj, S. K.; Sharma, H. K.; Mairesse, G.; Barbier, P.; Nowogrocki, G. *J. Chem. Soc., Dalton Trans.* **1988**, 1719.
(29) Swisher, R. G.; Vollano, J. F.; Chandrashekhar, V.; Day, R. O.; Holmes, R. R. *Inorg. Chem.* **1994**, *23*, 3147.

Table 1. Analytical and Physical Data for **1**−**4**

compound	% yield	mp (°C)	elemental analysis[a] (%) C	H	N	pH[b] (concentrated)
1	65	>250	56.87 (56.70)	4.25 (4.08)	9.45 (9.45)	*c*
2	80	250 (dec)	45.93 (45.90)	5.05 (4.95)	7.97 (7.65)	7.22 (1.99×10^{-2})
3	85	>280 (dec)	40.68 (40.62)	4.45 (4.38)	7.14 (6.77)	5.87 (7.01×10^{-3})
4	72	>270 (dec)	39.73 (39.33)	3.29 (3.30)	6.77 (6.55)	6.05 (1.34×10^{-2})

[a] Calculated values in parentheses. [b] In water as solvent. [c] Poor solubility.

to several known magnesium complexes wherein Mg^{2+} ion preferentially binds to water molecules, often in the form of $[Mg(OH_2)_6]^{2+}$.[30]

Table 1 also lists the measured pH values of the dilute solutions of the new complexes. While the aqueous solution of the calcium complex is almost neutral (pH = 7.22), the solutions of the strontium and barium complexes were found to be slightly acidic. Any further dilution of these solutions does not appreciably change the observed pH values. While the complexes **3** and **4** show acidic pH values (5.87 and 6.05) due to the coordination of one of the $-NH_2$ groups to the metal ion, the observed neutral pH for **2** is consistent with the free $-NH_2$ groups present in the complex.

Spectral Characterization. Products **1**−**4** were further characterized by UV, IR, and ^1H NMR (Table 2) spectral studies. The UV spectra of **1**−**4** in water or methanol as the solvent medium contain three strong absorption maxima (e.g., 209, 238, and 310 nm for **2** in H_2O). However, the spectra recorded in DMSO show only two peaks (e.g., 261 and 323 nm for **2**). The observed spectral data are very similar to the values observed for the free ligands in the respective solvents, suggesting that the transitions observed in all cases are essentially ligand-based. This observation suggests that in dilute solutions, the complexes are probably dissociated into $[M(H_2O)_6]^{2+}$ and anthranilate anions.[21]

The observed IR spectra as KBr plates are also depicted in Figure 1. While complexes **2**−**4** have a broad but strong absorption at 3400−3500 cm^{-1} corresponding to the presence of water molecules in the complex, the IR spectrum of **1** is devoid of any absorption beyond 3310 cm^{-1}, which clearly indicates the absence of any sort of water molecule in the complex. Hill and Curran interpret the absorption at around 3500 cm^{-1} to the N−H stretching frequency of the amino group after coordination to the metal. However, on the basis of our X-ray

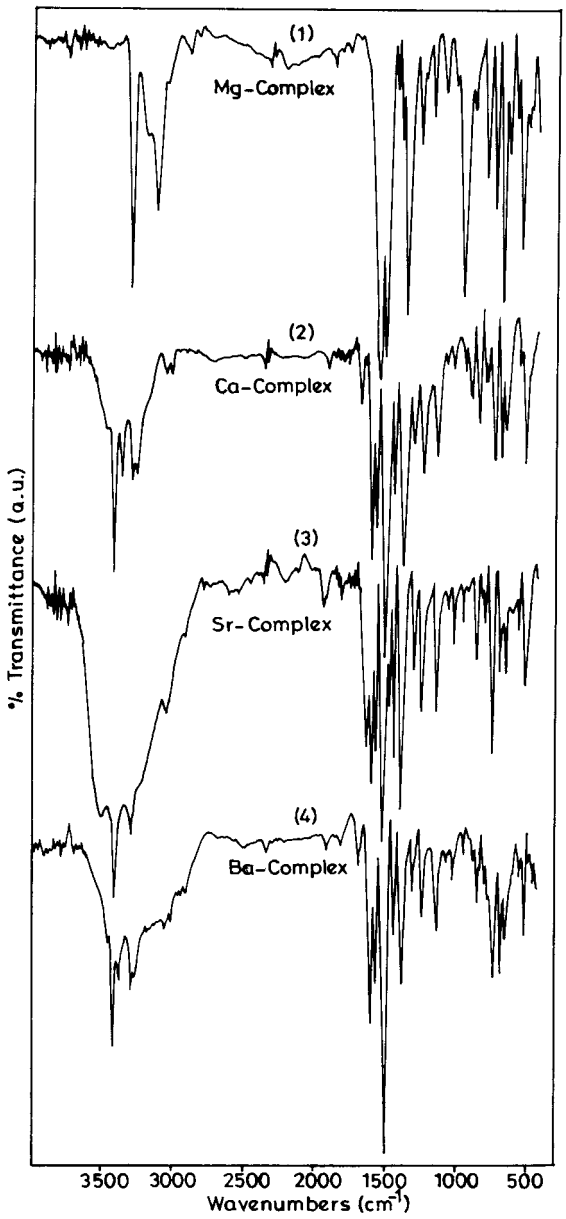

Figure 1. Observed IR spectra of complexes **1**−**4** as KBr plates.

Table 2. ^1H and ^{13}C NMR Spectral Data for **1**−**4** for Spectral Assignments (See Figure 3)[a]

compound	^1H NMR δ (H_b), ppm (J, Hz)	δ (H_c) ppm (J, Hz)	δ (H_d), ppm (J, Hz)	δ (H_e), ppm (J, Hz)	^{13}C NMR δ, ppm
2-abaH	6.71	7.27	6.62	7.86	
1[b]	6.57	7.06 ($^4J_{HcHe} = 1.7$)	6.40 ($^4J_{HdHb} = 1.0$)	7.77 ($^3J_{HeHd} = 6.9$)	*c*
2[d]	6.69 ($^3J_{HbHc} = 8.1$) ($^4J_{HbHd} = 1.2$)	7.12 ($^3J_{HcHb} = 8.5$) ($^3J_{HcHd} = 6.8$) ($^4J_{HcHe} = 1.4$)	6.57 ($^3J_{HdHc} = 8.1$) ($^3J_{HdHe} = 6.9$) ($^4J_{HdHb} = 1.0$)	7.9 ($^3J_{HeHd} = 7.9$) ($^4J_{HeHc} = 1.7$)	178.24(C_a), 132.81(C_b), 117.82(C_c), 117.25(C_d), 119.75(C_e), 133.06(C_f), 151.02(C_g)
3[d]	6.69 ($^3J_{HbHc} = 8.2$) ($^4J_{HbHd} = 1.1$)	7.12 ($^3J_{HcHb} = 8.0$) ($^3J_{HcHd} = 7.0$) ($^4J_{HcHe} = 1.6$)	6.57 ($^4J_{HdHb} = 1.0$)	7.8 ($^3J_{HeHd} = 7.7$) ($^4J_{HeHc} = 1.6$)	177.76(C_a), 132.64(C_b), 117.84(C_c), 117.17(C_d), 119.40(C_e), 133.84(C_f), 152.12(C_g)
4[d]	6.69 ($^3J_{HbHc} = 8.1$) ($^4J_{HbHd} = 0.9$)	7.10 ($^3J_{HcHb} = 8.4$) ($^3J_{HcHd} = 6.8$) ($^4J_{HcHe} = 1.4$)	6.58 ($^3J_{HdHc} = 7.8$) ($^3J_{HdHe} = 6.9$) ($^4J_{HdHb} = 1.1$)	7.79 ($^3J_{HeHd} = 7.8$, $^4J_{HeHc} = 1.4$)	177.42(C_a), 132.45(C_b), 117.89(C_c), 117.37(C_d), 121.01(C_e), 132.63(C_f), 150.70(C_g)

[a] Spectra of **1**, **2**, and **4** were recorded at 200 MHz and spectrum of **3** at 400 MHz. [b] DMSO-d_6 as solvent. [c] Poor solubility. [d] CD_3OD as solvent.

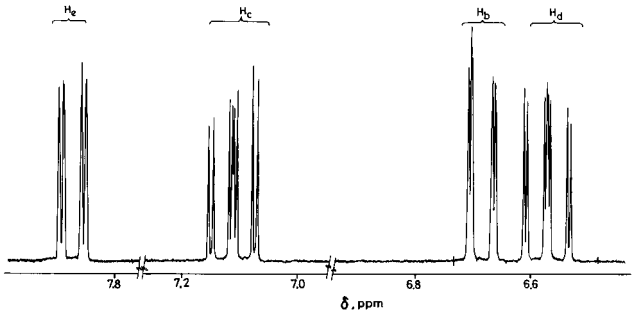

Figure 2. Aromatic region of the ^{1}H NMR spectrum of **2** recorded in CD_3OD at 200 MHz.

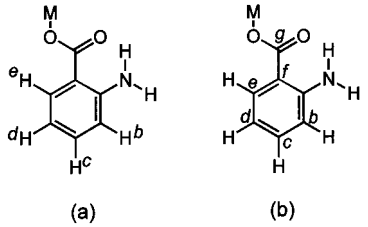

Figure 3. Labeling scheme for the NMR assignments: (a) ^{1}H NMR; (b) ^{13}C NMR.

structural studies (vide infra) and the solid-state IR spectral studies, we believe that the absorption around 3500 cm^{-1} is most likely due to the water molecules. For example, although there is no coordination of the $-NH_2$ group to the metal in **2**, the observed spectra in this region for both complexes **2** and **3** are very similar. Moreover, even in complexes **3** and **4** where the $-NH_2$ coordination is observed, it is only one of the anthranilate ligands that is involved in the amino coordination. Hence, if this absorption were really due to the NH_2 group, one would expect an entirely different absorption pattern in the 3200−3500 cm^{-1} for all three complexes (Figure 1).

The high-field ^{1}H NMR spectra of complexes of **1**−**4** show very similar behavior (Table 2). The observed spectrum for **2** in the aromatic region is shown in Figure 2. Because of the poor solubility of the complex in $CDCl_3$, the spectra for **2**−**4** were recorded in CD_3OD while it was possible to obtain the spectrum of **1** only in $(CD_3)_2SO$. As expected, four sets of signals are observed in the aromatic region for the four different aryl protons b−e (see Figure 3a). The resonance of all the protons are slightly high-field-shifted compared to the corresponding values found for 2-abaH. The H_b proton in **1**−**4**, which is ortho to the amino group, couples with both H_c and H_d protons to varying extents and results in a doublet of a doublet at around δ 6.6−6.7 ppm with J values of 8 and 1 Hz, respectively. The H_c proton is involved in a three-bond coupling with H_b and H_d (J = 8 and 7 Hz, respectively) in addition to a weak four-bond coupling with H_e (J = 1.5 Hz). Similarly, proton H_d also shows a doublet of a doublet of a doublet resulting from two three-bond and one four-bond coupling with H_c and H_e and H_b protons (J = 8, 7, and 1 Hz, respectively). As expected, the proton H_e is downfield-shifted because of its presence in the vicinity of a carboxylate group (δ = 7.8 ppm) and appears as a doublet of a doublet because of the three-bond coupling with H_d and four-bond coupling with H_c.

The ^{13}C NMR spectra of complexes **2**−**4** in CD_3OD show seven different resonances between 115 and 180 ppm for the seven different carbon atoms that are present in the anthranilate ligand (Table 2, Figure 3b). The highfield shifts of 117.3, 117.8, and 119.8 ppm in **2** are easily assignable to the C_d, C_c, and C_e, respectively, while the low-field shift at 178.2 ppm is due to carbon atom C_a, which is attached to the amino group. The carboxyl carbon atom C_g resonates at 151.0 ppm.

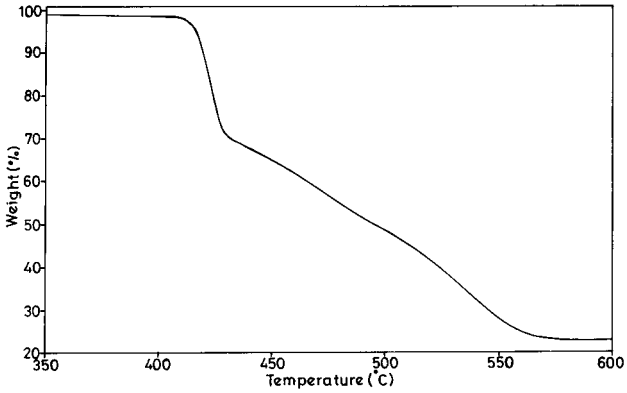

Figure 4. TGA plot of **1** (in N_2) showing no weight loss below 400 °C.

Thermal Analysis. Thermal analyses for all the products have been carried out to clearly establish the content of coordinated and uncoordinated water molecules in the complexes. As expected from its analytical data, the magnesium anthranilate complex **1** (Figure 4) does not show any weight loss up to 412 °C, indicating the absence of any coordinated or lattice water molecules in the complex. The first weight loss for **1** occurs from 412 to 428 °C, which approximately corresponds to the loss of two carbon dioxide molecules. However, in the case of calcium complex **2**, the first weight loss occurs between 43 and 140 °C corresponding to the loss of three water molecules, which is consistent with our formulation for this compound based on the analytical data (vide supra). The second weight loss for **2** is observed between 304 and 453 °C corresponding to the loss of two carbon dioxide molecules. A very similar thermal behavior is also observed for the strontium anthranilate **3**.

In the case of barium complex **4**, six weight losses in the temperature region 160−170, 170−195, 195−215, 295−415, 415−504, and 504−570 °C have been observed. The first transition amounting to 4% weight loss corresponds to the loss of the only coordinated water molecule. While the origins of the second, third, and fourth transitions are unclear, the material left after the fifth transition, corresponding to 47% weight of the original material, can be easily attributed to the formation of $BaCO_3$. The final transition occurring between 504 and 570 °C converts $BaCO_3$ into BaO. However, in the case of complexes **1**−**3**, even after heating until 600 °C, only metal carbonates were obtained.

Although it has been possible to derive the exact composition and to some extent the structural formula of all the compounds from the analytical, spectroscopic, and thermal analysis data, the obtained information is insufficient to establish the actual modes of binding of the ligands to the metal ions. Moreover, the presence of $-NH_2$ and $-COO^-$ groups leads to associated structures in the solid state through extensive hydrogen bonding. Hence, to have a clear understanding of the structures of these compounds, detailed X-ray structural investigations have been carried out for compounds **2**−**4**, and the results are described below. Our repeated attempts to obtain suitable single crystals for Mg anthranilate **1** have so far been unsuccessful.

Crystal Structure of $[Ca(2\text{-aba})_2(OH_2)_3]_\infty$ (2). The thermal ellipsoid plot of $[Ca(2\text{-aba})_2(OH_2)_3]_\infty$ (**2**) showing the immediate coordination environment around the central metal ion is shown

(30) For example, the reaction of 4-aminobenezoic acid with $MgCl_2$ forms $[Mg(H_2O)_6]^{2+}$ 2[4-aminobenzoate]$^-$; see ref 31.

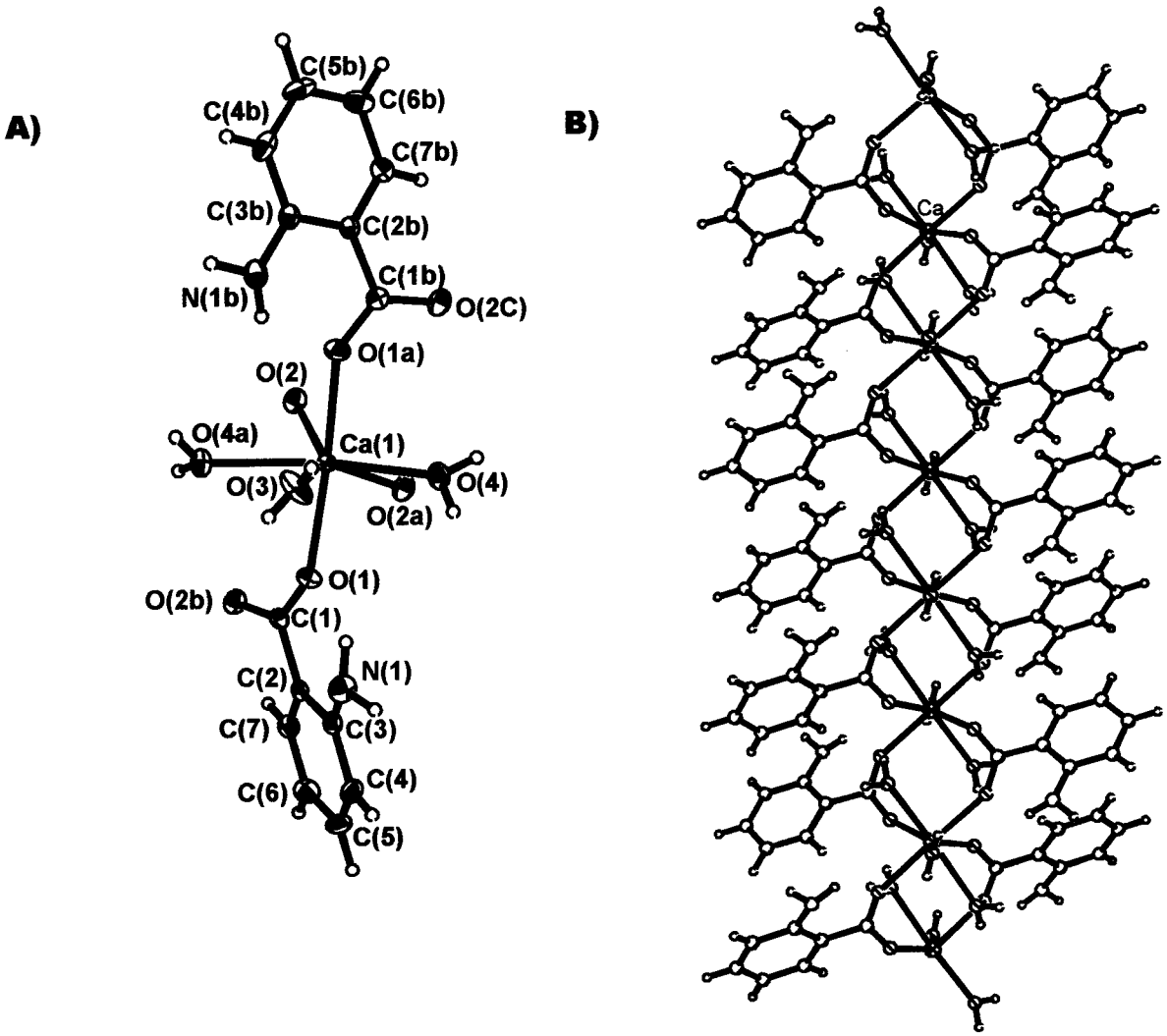

Figure 5. (A) Thermal ellipsoid plot of **2** drawn at 50% probability level. (B) Diagram depicting the formation of a one-dimensional polymeric chain.

Table 3. Bond Lengths [Å] and Angles [deg] for **2**[a]

Ca(1)−O(1A)	2.326(1)	Ca(1)−O(1)	2.326(1)
Ca(1)−O(2)	2.373(1)	Ca(1)−O(2A)	2.373(1)
Ca(1)−O(3)	2.408(2)	Ca(1)−O(4A)	2.485(1)
Ca(1)−O(4)	2.485(1)	N(1)−C(3)	1.398(2)
O(3)···O(4B	2.964(2)	O(4)···O(2C)	2.800(2)
O(4)···N(1D)	3.061(2)	C(7)···O(1E)	3.614(2)
O(1A)−Ca(1)−O(1)	163.9(7)	O(1A)−Ca(1)−O(2)	79.2(5)
O(1)−Ca(1)−O(2)	114.2(5)	O(1A)−Ca(1)−O(2A)	114.2(5)
O(1)−Ca(1)−O(2A)	79.2(5)	O(2)−Ca(1)−O(2A)	74.4(6)
O(1A)−Ca(1)−O(3)	81.9(4)	O(1)−Ca(1)−O(3)	81.9(4)
O(2)−Ca(1)−O(3)	142.8(3)	O(2A)−Ca(1)−O(3)	142.8(3)
O(1A)−Ca(1)−O(4A)	94.0(5)	O(1)−Ca(1)−O(4A)	81.5(5)
O(2)−Ca(1)−O(4A)	76.0(5)	O(2A)−Ca(1)−O(4A)	133.6(5)
O(3)−Ca(1)−O(4A)	73.7(4)	O(1A)−Ca(1)−O(4)	81.5(5)
O(1)−Ca(1)−O(4)	94.0(5)	O(2)−Ca(1)−O(4)	133.6(5)
O(2A)−Ca(1)−O(4)	76.0(5)	O(3)−Ca(1)−O(4)	73.7(4)
O(4A)−Ca(1)−O(4)	147.4(7)	O(3)−H(3a)···O(4B)	158(2)
O(4)−H(4b)···O(2C)	163(3)	O(4)−H(4a)···N(1D)	163(3)
C(7)−H(2)···O(1E)	170(2)		

[a] Symmetry transformations used to generate equivalent atoms. A: $-x, y, -z + 1/2$. B: $-x, -y + 1, -z$. C: $-x, -y, -z$. D: $x, -y + 1, +z - 1/2$. E: $x, -y, +z + 1/2$.

in Figure 5. Selected bond lengths and angles are listed in Table 3. The compound crystallizes in the centrosymmetric orthorhombic group *Pbcn*. The calcium atoms in **2** are heptacoordinated, in contrast to the observed eight coordination in the closely related 4-aba complex of calcium[31] and [Ca(4-aminosalicylate)(acetate)(H_2O)]·H_2O.[17] Four of the coordination sites in **2** are occupied by bridging carboxylate oxygen atoms (O(1), O(1A), O(2), O(2A)). To complete the coordination sphere, each calcium atom is further complexed to three water molecules (O(3), O(4), O(4A)). The net result is the formation of an eight-membered ring ($Ca_2C_2O_4$) between every adjacent calcium atom, which also leads to the formation of a one-dimensional polymeric chain of calcium atoms (see Figure 5). The amino group of the anthranilate ligand does not directly take part in the coordination to the metal but forms a hydrogen bond with the oxygen atom of a coordinated water molecule from a neighboring polymeric chain (Table 3). In addition, O−H···O hydrogen bonds exist between the polymeric chains that originate from either the coordinated water molecules or the carboxylate oxygen atoms. Thus, the one-dimensional polymeric chains are connected to each other, resulting in the formation of a supramolecular metal−organic framework as shown in Figure 6. The distance of 4.699(1) Å between the neighboring calcium atoms along the chain is much longer than the observed value of 4.05 Å between the calcium atoms in the case of the related complex [Ca(4-aminosalicylate)(acetate)-(H_2O)]H_2O.[17]

(31) Murugavel, R.; Karambelkar, V. V.; Anantharaman, G. *Indian J. Chem., Sect. A*, in press.

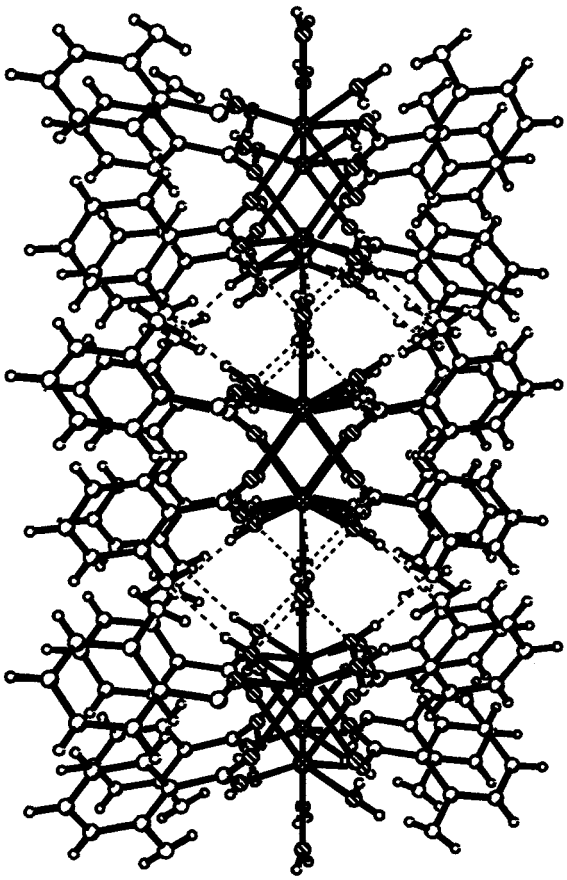

Figure 6. Packing plot of the polymeric chains of **2** in crystal resulting in hydrogen-bonded supramolecular structure.

The coordination geometry around the calcium atom can at best be described as heavily distorted pentagonal bipyramidal, with a large deviation from the mean plane of the pentagon. The pyramidal positions are occupied by O(1) and O(1A) with a trans angle of 163.9°. The angles around calcium vary from 73.7 to 163.9°. The Ca−O distances range from 2.326(1) to 2.485(1) Å. The longer distances are those arising from coordinated water molecules, while the shorter distances are due to the carboxylate oxygen atoms. There is a small difference between the Ca−O(1) and Ca−O(2) distances. The Ca−O distances in **2** are comparable to those found in the case of related carboxylate complexes.[32]

Crystal Structure of [{Sr(2-aba)$_2$(OH$_2$)$_2$}·H$_2$O]$_\infty$ (3). The thermal ellipsoid plot of [{Sr(2-aba)$_2$(OH$_2$)$_2$}·H$_2$O]$_\infty$ (**3**) showing the immediate coordination environment around the central metal ion is shown in Figure 7. Selected bond lengths and angles are listed in Table 4. The compound crystallizes in the monoclinic noncentrosymmetric space group C_2. Despite identical elemental composition (other than the central metal), the solid-state structures of calcium and strontium complexes **2** and **3** completely differ from each other. For example, the strontium atoms in **3** are nine-coordinated with a weak metal−metal interaction. Each strontium atom is coordinated by five carboxylate oxygen atoms, three water molecules, and an amino group. While the anthranilate ligands in calcium complex **2** act only as a bridging ligand through their carboxyl functionality, the two types of anthranilate ligands in **3** show an entirely different coordinating behavior. The mode of coordination of each of these types of ligands is depicted in Figure 8. Thus, like in **2**, strontium atoms in **3** also form a zigzag polymeric chain with the help of these two contrastingly different anthranilate ligands. The most important observation to note here is the ability of the amino group of one of the anthranilate ligands to take part in coordination with a neighboring strontium atom, while the amino group of the other anthranilate ligand is involved in only hydrogen-bonding interactions as in the case of **2**. However, the hydrogen-bonding interaction in **3** becomes more complex because of the presence of an additional lattice water molecule apart from the three-coordinated water molecules. There are as many as nine different O−H···O, N−H···O, C−H···O hydrogen bonds that are responsible for the supramolecular assembly depicted in Figure 9.

The 36 different bond angles around the nona-coordinated strontium atom vary over a wide range (46.5(1)−148.7(2)°). The smallest bond angle of 46.5(1)° involves the chelating oxygen atoms O(1) and O(2). Quite expectedly, the Sr−O distances also vary over a vast range (2.490(6)−2.926(6) Å). The shortest distance of 2.490(6) Å corresponds to the oxygen atom O(3), which is coordinated to the metal in a monodentate fashion. Although the C(1)−O(1) and C(11)−O(2) distances of 1.238(9) and 1.265(9) Å are indicative of full delocalization of the carboxylate negative charge, the Sr(1)−O(1) and Sr(1)−O(2) distances differ considerably (2.926(6) and 2.599(5) Å, respectively). An interesting structural feature in **3** is the rather short Sr···Sr distance of 3.92 Å. The two N−C distances in the molecule are nonequal because of the fact that one of the amino groups is coordinated to the strontium metal (N(2)−Sr(1) 3.055(9) Å) while the other amino group remains uncoordinated. Thus, the C(3)−N(1) distance (1.395(11) Å) is considerably shorter than the C(13)−N(2) distance (1.439(14) Å). In general, the coordination geometry, Sr−O distances, and O−Sr−O angles in **3** are comparable to those found in the [Sr(L-glutamate)·6H$_2$O] complex reported by Schmidbaur et al.[14] and other Sr−carboxylate complexes.[32,33] However, no amino coordination was found in the glutamate complex as in the case of **2**.

Crystal Structure of [Ba(2-aba)$_2$(OH$_2$)]$_\infty$ (4). The molecular structure of [Ba(2-aba)$_2$(OH$_2$)]$_\infty$ (**4**) showing the immediate coordination environment around the central metal ion and the thermal motions of the atoms is shown in Figure 10. Selected bond lengths and angles are listed in Table 5. The compound crystallizes in the orthorhombic centrosymmetric space group *Pbcn*. The barium atoms in **4** are nine-coordinated as in the case of the strontium atom in **3**. However, the coordination environment around the barium atom varies significantly compared to that found in **3**. Each barium atom is coordinated by six carboxylate oxygen atoms, two bridging water molecules, and one amino group. Two chelate rings are found around each barium atom; the first is a four-membered chelate ring formed by the carboxylate group of one of the anthranilate ligands, while the second is a six-membered chelate ring that is formed by the carboxyl atom O(1) and the amino nitrogen N(1). Apart from this chelating function of the two anthranilate ligands, they are also engaged in bridging the neighboring barium atoms. The exact modes of coordination of these ligands are represented in Figure 11. Thus, the carboxylate oxygen atoms O(1) and O(3) bridge the barium atom along the chain, and the other carboxylate oxygen O(2) is involved in bridging the barium atoms from an adjacent chain. The net result is the formation of a two-dimensional polymer that has been, for simplicity's sake, schematically represented in Figure 12. The water molecule O(5)

(32) Poonia, N. S.; Bajaj, A. V. *Chem. Rev.* **1979**, *79*, 389.

(33) (a) Briaggman, B.; Oskarsom, A. *Acta Crystallogr., Sect B* **1977**, *33*, 1900. (b) Palmer, K. J.; Wong, R. Y.; Lewis, J. C. *Acta Crystallogr., Sect B* **1972**, *28*, 223.

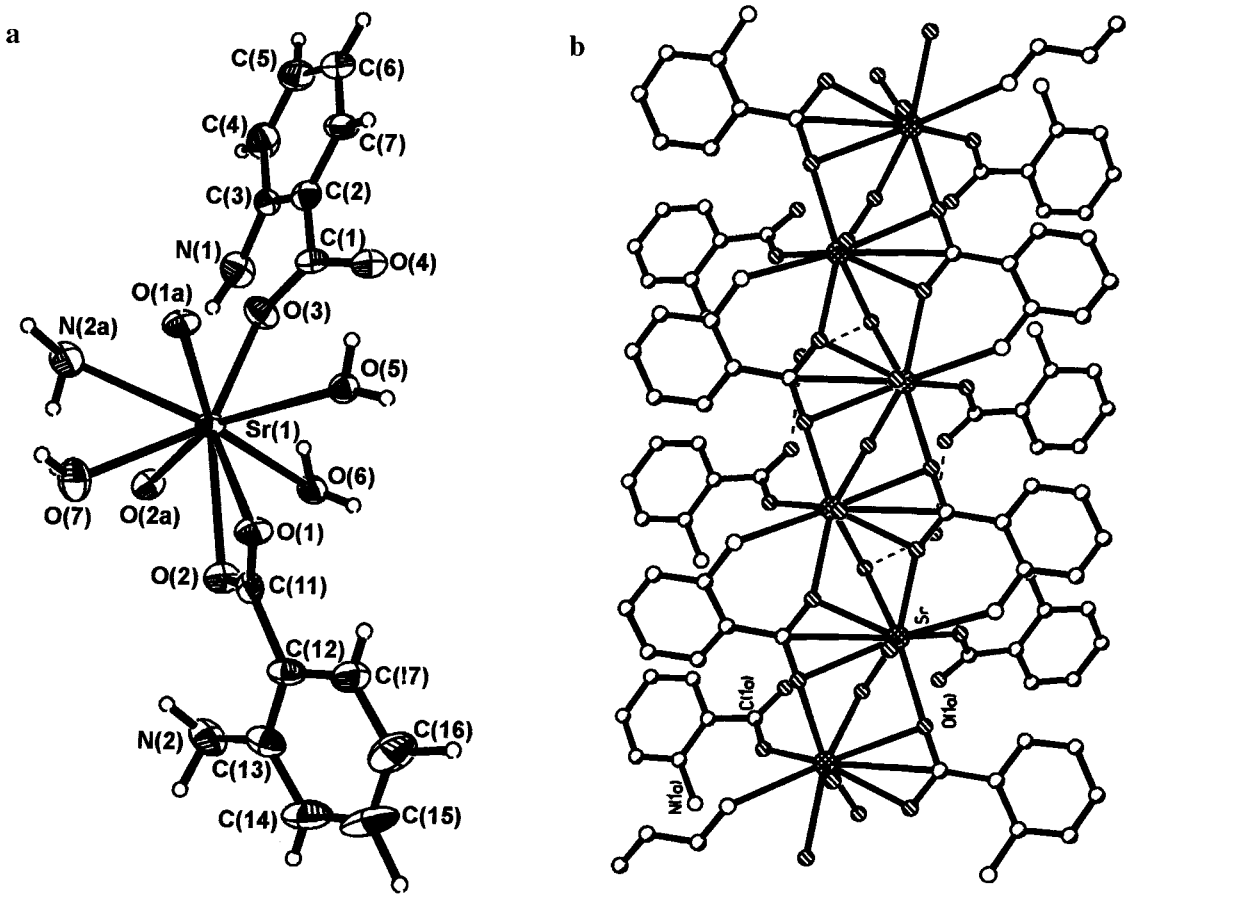

Figure 7. (a) Thermal ellipsoid plot of **3** drawn at 50% probability level. (b) Plot of the one-dimensional polymeric chain in **3**.

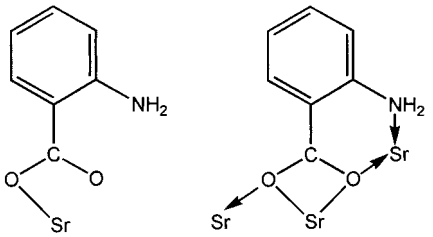

Figure 8. Schematic diagram of the coordination behavior of the two anthranilate ligands in **3**.

bridges the two adjacent barium atoms along the polymeric chain. Because of the coordinated water molecules and the coordinated and free amino groups, a few hydrogen bonds are found in the solid state. However, these hydrogen bonds are formed within a given 2-D polymer and do not extend the coordination polymer network to a 3-D supramolecular assembly.

The bond angles around the barium varies from 44.6(1) to 148.6(1)°. Similarly, the Ba−O distances also vary from 2.670-(3) to 3.012(4) Å. The two N−C distances in the molecule are nonequal, since only one of the amino groups is coordinated to the barium metal. The N(1)−Ba(1) distance in **4** (3.047(4) Å) is somewhat shorter than the N−Sr distance found in **3** despite the larger size of barium, indicating that the amino group is more firmly bound in the case of **4**. In general, the coordination geometry and the metric parameters in **4** are comparable to those found in several carboxylate complexes of barium containing additional macrocyclic ligands[17,32,34] and that of the Ba(L-Glu)·$6H_2O$ complex.[14] As in the case of **3**, short Ba···Ba distances of are found in **4** (4.32 Å).

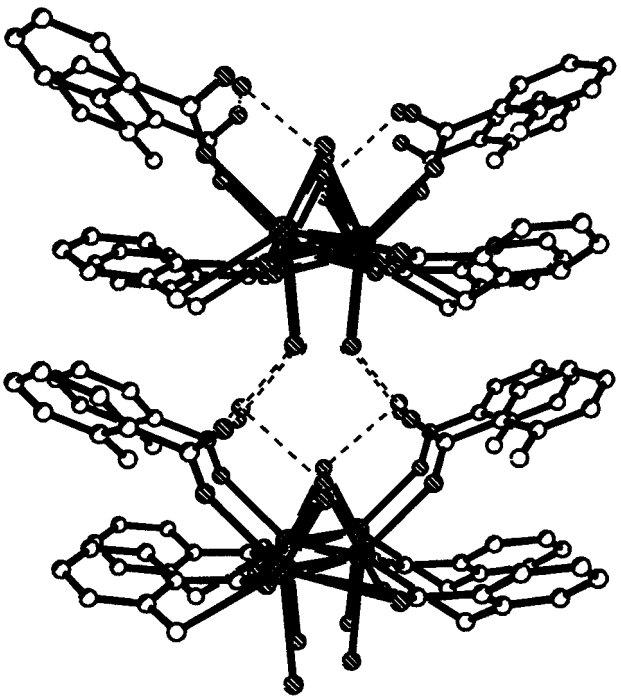

Figure 9. Packing diagram showing the stacking of the polymeric chains of **3**.

Conclusions

The present investigation demonstrates that for a given M/L ratio, the coordinating ability of the anthranilic acid can be fine-

(34) (a) Voegele, J. C.; Thierry, J. C.; Weiss, R. *Acta Crystallogr., Sect B* **1974**, *30*, 70. (b) Burns, J. H.; Musikas, C. *Inorg. Chem.* **1977**, 1619.

Table 4. Selected Bond Lengths [Å] and Angles [deg] for **3**[a]

Sr(1)−O(3)	2.490(6)	Sr(1)−O(1A)	2.493(5)
Sr(1)−O(2B)	2.531(5)	Sr(1)−O(2)	2.599(5)
Sr(1)−O(5)	2.615(6)	Sr(1)−O(7)	2.628(6)
Sr(1)−O(6)	2.702(6)	Sr(1)−O(1)	2.926(6)
Sr(1)−N(2B)	3.055(9)	Sr(1)−C(11)	3.119(8)
Sr(1)−Sr(1A)	3.918(2)	Sr(1)−Sr(1B)	3.924(2)
O(1)−Sr(1A)	2.493(5)	N(1)−C(3)	1.395(1)
O(2)−Sr(1B)	2.531(5)	N(2)−C(13)	1.439(1)
N(2)−Sr(1B)	3.055(9)	O(5)−Sr(1A)	2.615(6)
O(6)−Sr(1B)	2.702(6)	O(5)···O(4)	2.710(8)
O(6)···O(3)	3.235(6)	O(8)···O(4)	2.726(9)
N(2)···O(8C)	3.43(1)	O(5)···O(4A)	2.710(8)
O(5)···O(3A)	3.176(7)	O(6)···O(8A)	2.836(9)
C(17)···O(3A)	3.64(1)	O(7)···O(4D)	2.852(8)
O(8)···N(1E)	3.06(1)		

O(3)−Sr(1)−O(1A)	85.8(2)	O(3)−Sr(1)−O(2B)	94.0(2)
O(1A)−Sr(1)−O(2B)	140.5(2)	O(3)−Sr(1)−O(2)	143.6(2)
O(1A)−Sr(1)−O(2)	125.7(2)	O(2B)−Sr(1)−O(2)	73.4(2)
O(3)−Sr(1)−O(5)	76.9(2)	O(1A)−Sr(1)−O(5)	69.8(2)
O(2B)−Sr(1)−O(5)	148.4(2)	O(2)−Sr(1)−O(5)	95.9(1)
O(3)−Sr(1)−O(7)	140.2(2)	O(1A)−Sr(1)−O(7)	77.9(2)
O(2B)−Sr(1)−O(7)	77.4(2)	O(2)−Sr(1)−O(7)	71.5(2)
O(5)−Sr(1)−O(7)	128.3(2)	O(3)−Sr(1)−O(6)	77.0(2)
O(1A)−Sr(1)−O(6)	148.7(2)	O(2B)−Sr(1)−O(6)	67.5(2)
O(2)−Sr(1)−O(6)	66.6(2)	O(5)−Sr(1)−O(6)	80.9(2)
O(7)−Sr(1)−O(6)	131.1(2)	O(3)−Sr(1)−O(1)	140.3(2)
O(1A)−Sr(1)−O(1)	82.5(2)	O(2B)−Sr(1)−O(1)	118.6(2)
O(2)−Sr(1)−O(1)	46.5(2)	O(5)−Sr(1)−O(1)	63.4(2)
O(7)−Sr(1)−O(1)	73.4(2)	O(6)−Sr(1)−O(1)	94.3(1)
O(3)−Sr(1)−N(2B)	77.4(2)	O(1A)−Sr(1)−N(2B)	84.7(2)
O(2B)−Sr(1)−N(2B)	57.1(2)	O(2)−Sr(1)−N(2B)	118.9(2)
O(5)−Sr(1)−N(2B)	144.8(2)	O(7)−Sr(1)−N(2B)	65.2(2)
O(6)−Sr(1)−N(2B)	116(2)	O(1)−Sr(1)−N(2B)	138.3(2)
O(5)−H5B···O(4)	153(1)	O(6)−H6B···O(3)	152(8)
O(8)−H8B···O(4)	173(5)	N(2)−H2A···O(8C)	146(9)
O(5)−H5A···O(4A)	142(1)	O(5)−H5A···O(3A)	143(10)
O(6)−H6A···O(8A)	168(1)	C(17)−H17···O(3A)	168(8)
O(7)−H7B···O(4D)	161(1)	O(8)−H8A···N(1E)	169(6)

[a] Symmetry transformations used to generate equivalent atoms. A: $-x, +y, -z+1$. B: $-x, +y, -z$. C: $-x, +y+1, -z+1$. D: $x, +y+1, +z$. E: $x, +y, +z+1$.

tuned depending on the nature and size of the group 2 metal ions in the study. While both the anthranilate ligands in **2** make only four bonds to the central calcium metal through the carboxylate oxygen atoms, the number of contacts are increased to six and seven in **3** and **4**, respectively. The amino group of the anthranilate ligands in **2** does not coordinate to the metal presumably because of the fact that the calcium dication is a harder acid (compared to strontium and barium) and that it has a smaller coordination sphere. Thus, five different modes of coordination of the anthranilate ligands have been realized for complexes **2**−**4**. Another interesting outcome of this study is the ability of the anthranilate ligands and the coordinated and lattice water molecules to engage themselves in intra- and intermolecular hydrogen bonding to form two- and three-dimensional supramolecular networks. This observation necessitates further investigation of this aspect in order to generate new modular metal−organic extended solids[35] consisting of transition metal ions and aminobenzoic acids.

Because of the very complex coordination behavior of the carboxylate ions, it is very difficult to glean any information from the observed symmetric and asymmetric ν(C═O) shifts in the IR spectra of complexes **1**−**4** and to predict the nature of carboxylate binding. Although we envisage an octahedral

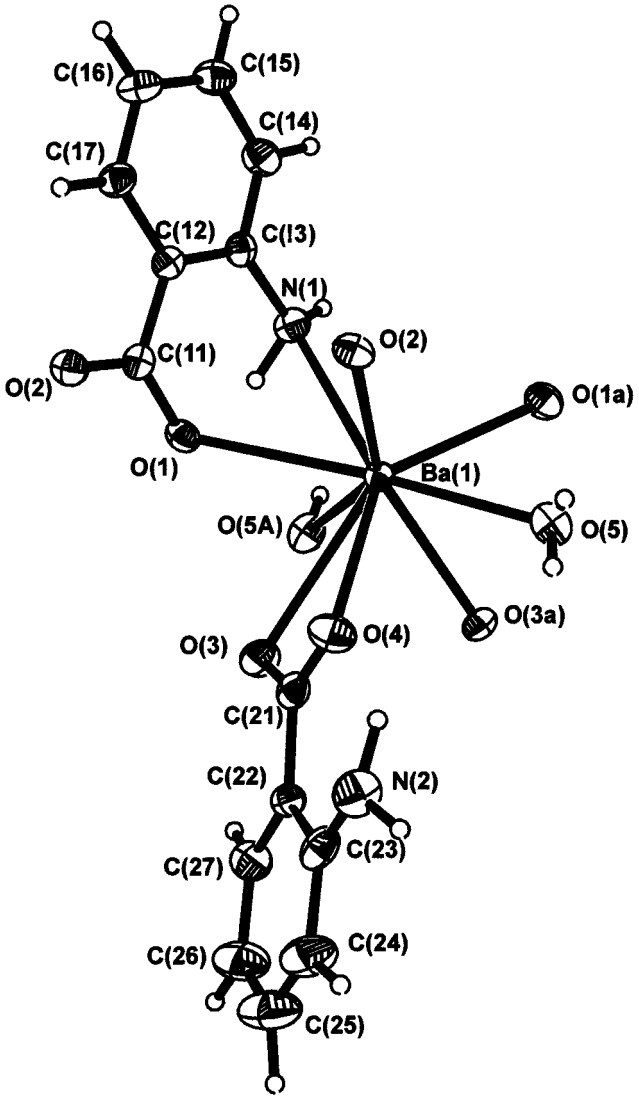

Figure 10. Thermal ellipsoid plot of **4** drawn at 50% probability level.

Mg^{2+} complex with the formula [Mg(2-aba)$_2$] for **1**, we are presently unable to assign a definitive structure to this compound with the available data. It appears that complex **1** might have a trans chelate square-planar base as suggested by Hill and Curran,[21] with two axial carboxylate carbonyls coordinating from either side of the square plane to make up a final octahedral geometry. An X-ray diffraction study for **1** will be crucial for making any further generalizations on the chemistry and the structural features of anthranilate complexes of divalent group 2 metal ions. Further work in our laboratory concentrates on the use of modified aminobenzoic acids and their derivatives to generate magnesium and calcium complexes, keeping in mind their possible applications in biology and medicinal chemistry.

Experimental Section

Instruments and Methods. Solvents were rigorously dried and routinely freshly distilled by standard methods prior to their use.[36] Deionized water used as solvent in all the reactions was doubly distilled prior to use. Starting materials were procured from commercial sources and used as received. Elemental analyses were performed on a Carlo Eraba (Italy) model 1106 elemental analyzer. The melting points were measured in glass capillaries and are uncorrected values. The ^{1}H and ^{13}C NMR spectra were recorded either on a Bruker AM 200 or on a

(35) For recent accounts on modular metal−organic extended solids, see the following. (a) Yaghi, O. M.; Li, H.; Davis, C.; Richardson, D.; Groy, T. L. *Acc. Chem. Res*. **1998**, *31*, 481. (b) Janiak, J. *Angew. Chem., Int. Ed. Engl*. **1997**, *36*, 1431.

(36) Perrin, D. D.; Armargeo, W. L. F. *Purification of Laboratory Chemicals*, 3rd ed.; Pergamon: London, 1988.

Table 5. Selected Bond Lengths [Å] and Angles [deg] for **4**[a]

Ba(1)−O(3A)	2.671(3)	Ba(1)−O(2B)	2.715(3)
Ba(1)−O(1A)	2.773(3)	Ba(1)−O(1)	2.783(3)
Ba(1)−O(4)	2.792(3)	Ba(1)−O(5)	2.882(6)
Ba(1)−O(5C)	2.906(5)	Ba(1)−O(3)	3.011(4)
Ba(1)−N(1)	3.047(4)	Ba(1)−Ba(1A)	4.317(8)
N1···N(2D)	3.177(6)	O5···O(4B)	2.854(6)
O5···O(3A)	3.018(7)		

O(3A)−Ba(1)−O(2B)	97.4(1)	O(3A)−Ba(1)−O(1A)	73.7(1)
O(2B)−Ba(1)−O(1A)	147.2(1)	O(3A)−Ba(1)−O(1)	138.0(1)
O(2B)−Ba(1)−O(1)	78.7(1)	O(1A)−Ba(1)−O(1)	129.1(1)
O(3A)−Ba(1)−O(4)	133.3(1)	O(2B)−Ba(1)−O(4)	85.7(1)
O(1A)−Ba(1)−O(4)	78.8(1)	O(1)−Ba(1)−O(4)	88.6(1)
O(3A)−Ba(1)−O(5)	65.7(1)	O(2B)−Ba(1)−O(5)	77.6(1)
O(1A)−Ba(1)−O(5)	69.8(1)	O(1)−Ba(1)−O(5)	148.6(1)
O(4)−Ba(1)−O(5)	69.5(1)	O(3A)−Ba(1)−O(5C)	97.7(1)
O(2B)−Ba(1)−O(5C)	145.5(1)	O(1A)−Ba(1)−O(5C)	67.2(1)
O(1)−Ba(1)−O(5C)	69.5(1)	O(4)−Ba(1)−O(5C)	105.5(1)
O(5)−Ba(1)−O(5C)	136.8(1)	O(3A)−Ba(1)−O(3)	141.2(1)
O(2B)−Ba(1)−O(3)	118.4(1)	O(1A)−Ba(1)−O(3)	68.1(1)
O(1)−Ba(1)−O(3)	68.5(1)	O(4)−Ba(1)−O(3)	44.6(1)
O(5)−Ba(1)−O(3)	105.9(1)	O(5C)−Ba(1)−O(3)	61.3(1)
O(3A)−Ba(1)−N(1)	83.7(1)	O(2B)−Ba(1)−N(1)	88.4(1)
O(1A)−Ba(1)−N(1)	120.9(1)	O(1)−Ba(1)−N(1)	54.5(1)
O(4)−Ba(1)−N(1)	143.0(1)	O(5)−Ba(1)−N(1)	144.0(1)
O(5C)−Ba(1)−N(1)	62.8(1)	O(3)−Ba(1)−N(1)	109.9(1)
Ba(1)−O(5)−Ba(1A)	96.5(1)		

[a] Symmetry transformations used to generate equivalent atoms. A: $^3/_2 - x$, $^3/_2 - y$, $^1/_2 + z$. B: x, $1 - y$, $^1/_2 + z$. C: $^3/_2 - x$, $^3/_2 - y$, $-^1/_2 + z$. D: $^3/_2 - x$, $^1/_2 + y$, z.

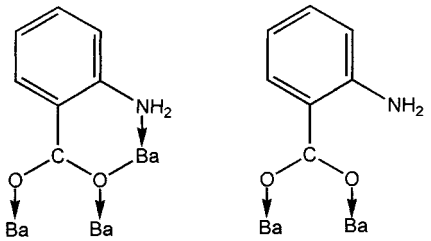

Figure 11. Schematic diagram of the coordination behavior of the two anthranilate ligands in **4**.

Bruker AS 400 instrument using Me_4Si as a reference for ^1H and ^{13}C spectral measurements. Infrared spectra were recorded on a Nicolet Impact 400 spectrometer either as Nujol mulls between KBr plates or as KBr diluted thin plates in the solid state. TGA and DTA measurements were carried out at RSIC, IIT−Bombay, on a DuPont thermal analyzer model 2100 under a stream of nitrogen gas.

Preparation of Complexes 1−4. Complexes **1**−**4** have been synthesized starting from the respective metal chlorides essentially by following a similar synthetic procedure. For example, $MCl_2 \cdot xH_2O$ (5 mmol) and anthranilic acid (10 mmol, 1.37 g) were dissolved in a H_2O (15 mL)/methanol (30 mL) mixture, and the resulting solution was warmed to 50 °C for 1 h. Aqueous NH_3 (25%) (20 mL) was added dropwise to this solution, and the resulting mixture was heated to 80 °C. A voluminous white precipitate formed in the reaction with $MgCl_2 \cdot 6H_2O$, was separated by filtration, and was dried in air to yield analytically pure **1**. In other cases, the resulting turbid reaction mixture was filtered and allowed to stand at room temperature to obtain large crystals of **2**−**4** after ∼48 h.

The magnesium derivative **1** was also obtained in good yield by using NaOH in place of aqueous ammonia. Similarly, the barium derivative **4** is also accessible in about 70% yield by starting from barium acetate without the use of any added base. The isolated yield, melting point, analytical data, and the solution pH values for complexes **1**−**4** are listed in Table 1. The ^1H and ^{13}C NMR spectral data are given in Table 2. The IR and visible spectral data are provided as Supporting Information.

X-ray Structure Determination Procedure. Single crystals of **2**−**4** were grown from a dilute water/methanol solution at room temperature by slow evaporation over a period of several days. Crystals suitable for X-ray diffraction studies were chosen from these crops and mounted on a Siemens STOE AED2 four-circle diffractometer for the cell determination and intensity data collection. The unit cell parameters were derived and refined by using randomly selected reflections in the 2θ range 20−30°.

Other details pertaining to data collection and refinement are listed in Table 6. The intensity data of compounds **3** and **4** have been corrected for absorption effects using ψ data. The structures were solved by direct methods using SHELXS-86[37a] and refined by using SHELXL-97.[37b]

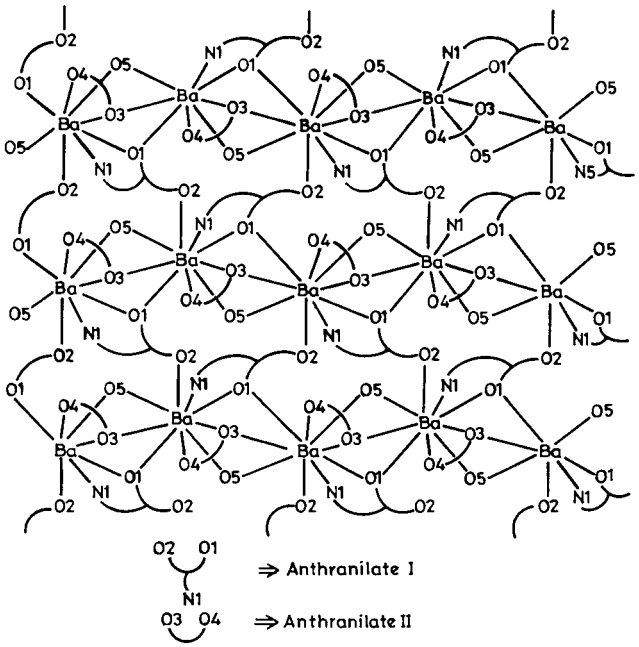

Figure 12. Schematic diagram of the coordination network in **4** showing the formation of the two-dimensional polymeric network.

Table 6. Crystal Data and Other Experimental Details for the Structure Determination of **2**−**4**

	2	**3**	**4**
empirical formula	$C_{14}H_{18}CaN_2O_7$	$C_{14}H_{18}N_2O_7Sr$	$C_{14}H_{14}BaN_2O_5$
fw	366.38	413.92	427.61
T, °C	150(2)	150(2)	200(2)
λ, Å	0.71073	0.71073	0.71073
crystal system	orthorhombic	monoclinic	orthorhombic
space group	*Pbcn*	C_2	*Pbcn*
a, Å	28.373(6)	32.020(6)	31.034(6)
b, Å	7.3176(15)	7.769(2)	12.134(2)
c, Å	7.9145(16)	6.895(1)	7.796(2)
β, deg		100.16(3)	
V, Å^3; Z	1643.2(6)	1688.3(6)	2936(1)
Z	4	4	8
ρ (calcd), g cm^{-3}	1.481	1.628	1.935
abs coeff, mm^{-1}	0.421	3.231	2.731
transm coeff		0.176, 0.305	0.236, 0.314
F(000)	768	840	1664
crystal size, mm	0.8 × 0.7 × 0.6	1.2 × 0.3 × 0.3	0.8 × 0.5 × 0.5
θ range	3.5−25.0	3.6−22.6	3.6−25.1
total reflns	2163	1303	8875
unique reflns	1431	1274	2599
goodness of fit on F^2	1.11	1.08	1.10
R_1 [$I > 2\sigma(I)$]	0.030	0.033	0.032
wR2 [$I > 2\sigma(I)$]	0.081	0.081	0.079
largest peak, e Å^3	0.262	0.558	0.874
largest hole, e Å^3	−0.341	−0.533	−1.126

(37) Sheldrick, G. M. *SHELXS-86: Program for Crystal Structure Solution*; University of Göttingen, Germany, 1986. (b) Sheldrick, G. M. *SHELXL-97: Program for Crystal Structure Refinement*; University of Göttingen, Germany, 1997.

All the hydrogen atoms in **4** were located from difference maps and were included in the refinement. While the hydrogen atoms attached to oxygen atoms in **3** and **4** were located from the difference maps (and their positions were refined), the hydrogen atoms attached to carbons atoms were geometrically fixed and refined using a riding model.

Acknowledgment. Financial support by CSIR, New Delhi (01(1546)/98/EMR-II) and DST, New Delhi (SP/S1/F19/98) for carrying out this work is gratefully acknowledged. The authors thank the RSIC, IIT—Bombay for the TGA and DTA measurements.

Supporting Information Available: Listings of IR, UV−vis, and X-ray data (including experimental details, atomic coordinates, complete bond lengths and angles, and anisotropic thermal parameters) for compounds **1**−**4**. This material is available free of charge via the Internet at http://pubs.acs.org.

IC990895K